

Polarization of the Cosmic Microwave Background from Non-Uniform Reionization

Guo-Chin Liu*, Naoshi Sugiyama[†], Andrew J. Benson**, C. G. Lacey[‡] and Adi Nusser[§]

**Institute of Astronomy and Astrophysics, Academia Sinica, Taiwan, R.O.C.*

[†]*Division of Theoretical Astrophysics, National Astronomical Observatory Japan, Mitaka, 181-8588, Japan*

***California Institute of Technology, MC 105-24, Pasadena, CA 91125, U.S.A.*

[‡]*SISSA, via Beirut 2-4, 34014 Trieste, Italy*

[§]*The Physics Department, The Technion-Israel Institute of Technology, Technion City, Haifa 32000, Israel*

Abstract. The secondary anisotropies and polarization of the Cosmic Microwave Background (CMB) provide a laboratory for the study of the epoch of reionization in the Universe. Here, we concentrate on the CMB *polarization* in models with inhomogeneous reionization. Although the amplitude of the polarization anisotropy is estimated to be much smaller than that in the temperature, it is advantageous to consider the polarization signal since it is generated when photons and electrons scatter for the last time. Detection of these signals will place important constraints on the reionization history of the Universe.

INTRODUCTION

Reionization produces interesting effects on CMB temperature and polarization anisotropies at both first and second order in the perturbations. At first order, the effects of reionization are the same as for an IGM with spatially uniform density and ionized fraction. Density fluctuations in the free electrons around the reionization epoch produce CMB anisotropies and polarization only at second order, as in the Vishniac effect [5]. These second-order anisotropies and polarization are small in amplitude, but nonetheless dominate over the first-order anisotropies on small angular scales of order of arc minutes. They are thus cosmologically interesting as a probe of structure present at reionization.

In this work, we concentrate on the second order polarization, which is generated by coupling of the temperature quadrupole with density fluctuations of the free electrons. In general, density fluctuations in the free electrons can be considered from two parts: one is the case of a homogeneous reionization of the IGM, with the fluctuations in the free electron density being assumed to follow the variations in the total matter density, the so-called “density modulation model”. Another case is that the reionization is expected to be patchy or inhomogeneous, with some regions already being fully ionized while others are still neutral, and the ionized regions growing until they encompass the whole IGM, the so-called “patchy reionization model”. Here, we consider a realistic reionization process by combining a semi-analytic model of galaxy formation with an N-body simulation of the distribution of dark matter in the universe to determine the distribution of ionized regions.

GALAXY FORMATION

The reionization history of the universe is determined by a semi-analytic model of galaxy formation. The semi-analytic model is that of Cole et al. (2000), which includes the following processes: formation and merging of dark matter halos through hierarchical clustering; shock-heating and radiative cooling of gas within these halos; collapse of cooled gas to form galactic disks; star formation in disks and feedback from supernova explosions; galaxy mergers; chemical evolution of the stars and gas; and luminosity evolution of stellar populations based on stellar evolution codes and model stellar atmospheres. The model has been shown by Cole et al. to agree fairly well with a wide range of observed properties of galaxies in the local universe. We used this model to calculate the ionizing luminosities of galaxies at

different redshifts, including the effects of absorption by interstellar gas and dust on the fraction of ionizing photons escaping, and followed the propagation of the ionization fronts around each galaxy. To find the ionizing luminosity, we first calculate the rate at which ionizing photons are being produced by stars in the galaxy, then apply an attenuation due to dust, and finally allow a fraction f_{esc} of the remaining photons to escape into the IGM. The mass of ionized hydrogen in each spherical ionization front is found by integrating the equation [4]

$$\frac{1}{m_{\text{H}}} \frac{dM}{dt} = S(t) - \alpha_{\text{H}}^{(2)} a^{-3} f_{\text{clump}} n_{\text{H}} \frac{M}{m_{\text{H}}}, \quad (1)$$

where n_{H} is the comoving mean number density of hydrogen atoms (total, HI and HII) in the IGM, m_{H} is the mass of a hydrogen atom, $a(t)$ is the scale factor of the universe normalized to unity at $z = 0$, t is time (related to the conformal time by $dt = d\tau/a$), $S(t)$ is the rate at which ionizing photons are being emitted and $\alpha_{\text{H}}^{(2)}$ is the recombination coefficient to levels $n \geq 2$. The clumping factor $f_{\text{clump}} \equiv \langle \rho_{\text{IGM}}^2 \rangle / \bar{\rho}_{\text{IGM}}^2$ gives the effect of clumping on the recombination rate of hydrogen in the IGM. A larger f_{clump} increases the recombination rate resulting in a delay of the reionization epoch. We use the clumping factor $f_{\text{clump}}^{(\text{halos})}$ as defined in Benson et al 2000. By summing over the ionized volumes due to all galaxies, we can calculate the fraction of the IGM which has been reionized at any redshift.

SECOND ORDER POWER SPECTRUM OF POLARIZATION

The second order polarization is generated by the coupling of *primary* temperature quadrupole with the density fluctuation of the free electrons. The density field of the gas is obtained by the simpler approach of Benson et al, in which the semi-analytic galaxy formation model is combined with a high-resolution N-body simulation of the dark matter. The simulation volume, which is a box of length $141.3h^{-1}\text{Mpc}$ and contains 256^3 dark matter particles each of mass $1.4 \times 10^{10} h^{-1} M_{\odot}$, is divided into 256^3 cubic cells. Then we determine which regions of the simulation box become ionized by using one of the five toy models A-E listed below, which span the likely range of possible behaviour.

Model A (Growing front model) Ionize a spherical volume around each halo with a radius equal to the ionization front radius for that halo calculated assuming a large-scale uniform IGM. Since in the simulation the IGM is *not* uniform, but is assumed to trace the dark matter, and also because some spheres will overlap, the ionized volume calculated in this way will not contain the correct total ionized mass. We therefore scale the radius of each sphere by a constant factor, f , and repeat the procedure. This process is repeated, with a new value of f each time, until the correct total mass of hydrogen has been ionized.

Model B (High density model) In this model, we ignore the positions of halos in the simulation. Instead, we simply rank the cells in the simulation volume by their density. We then completely ionize the gas in the densest cell. If this has not ionized enough HI then we ionize the second densest cell. This process is repeated until the correct total mass of HI has been ionized.

Model C (Low density model) This is like model B, except that we begin by ionizing the least dense cell, and work our way up to cells of greater and greater density.

Model D (Random spheres model) As Model A, except that the ionized spheres are placed at completely random positions in the simulation volume, rather than on the dark matter halos to which they belong. By comparing to Model A this model allows us to estimate the importance of the spatial clustering of dark matter halos.

Model E (Boundary model) Ionize a spherical region around each halo with a radius equal to the ionization front radius for that halo. This may ionize too much or not enough HI depending on the density of gas around each source. We therefore begin adding or removing cells at random from the boundaries of the already ionized regions until the required mass of HI is ionized.

In left panel of Fig. 1, we plot the second-order power spectrum of the polarization in the five toy models with fixed extreme escape fraction $f_{\text{esc}} = 1$ and $\Omega_b = 0.02$. The cosmological parameters are $\Omega_0 = 0.3$, $\Lambda_0 = 0.7$, Hubble constant $H_0 = 70 \text{ km/s/Mpc}$ and $\sigma_8 = 0.9$. We find reionization occurs at $z \sim 9$ (corresponding to the optical depth to reionization is 0.034) from semi-analytic model. Although the shapes of the curves are all very similar, their amplitudes are different. Note that the reduction in power above $l \sim 10,000$ is artificial and due to the limited resolution of the N-body simulation we use (the density field of the ionized gas is calculated on a grid with cell size $0.55h^{-1}\text{Mpc}$, corresponding to $l \sim 10^4$). On the other hand, the finite size of the simulation box ($256h^{-1}\text{Mpc}$) affects the power spectrum for l below a few hundred. We see that the amplitude of the power spectrum around the peak ($l \approx 10,000$) varies by a factor ≈ 2.5 , depending on which of the models A–E is used. The amplitude of the curves is affected by the

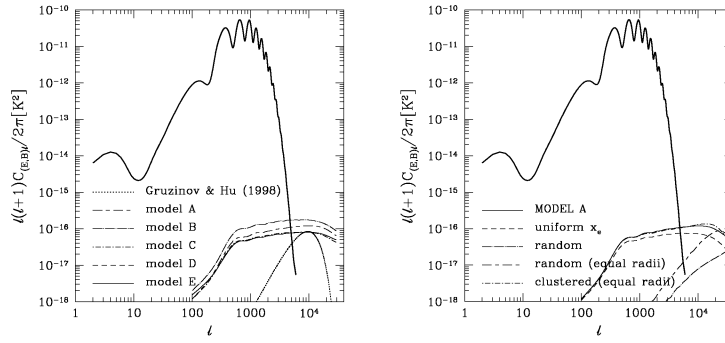


FIGURE 1. Power spectra of the second order effect for our models (left panel), and effect on the second-order anisotropy of varying the assumed geometry of the re-ionized regions (right panel).

strength of the correlations of δ_e present in each model. As a result, the “high density” model (B) is the most strongly correlated and has the highest amplitude, and conversely the “low density” model (C) has the lowest amplitude.

In left panel of Fig. 1, we also compare our results to the analytical toy model of Gruzinov & Hu (1998), in which the reionization is described by three free parameters. In their model, each luminous source is assumed to ionize a spherical region with fixed comoving radius R , the first source appears at redshift z_i , and new sources turn on at a constant rate until reionization is complete after an interval δz . An artificial assumption is made that luminous sources appear at random locations in space, so there are no correlations between the positions of the ionized spheres. Assuming that the spheres remain ionized forever, the fractional ionization increases with increasing number density of ionized spheres during δz until the universe is completely ionized. We chose $R = 0.85h^{-1}$ Mpc, $z_i=11$ and $\delta z = 5$ in the Gruzinov & Hu model to match the peak in the power spectrum of secondary *temperature* anisotropies predicted for our model E. For small l , little power is generated in the Gruzinov & Hu model because, by design, the patches are uncorrelated.

To further clarify what determines the *shape* of the second-order anisotropy spectrum in our models, we carried out the following additional tests. The first test was to force the ionized fraction x_e to be uniform and equal to the same mean value as before, so that fluctuations δ_e in the free electron density are then simply equal to fluctuations δ in the *total* density. In this case, the angular power spectrum has an almost identical shape to the model A. In the next two tests (labelled “random” in right panel of Fig. 1), the *total* gas density was forced to be uniform (i.e. we set $\delta = 0$), and put bubbles down at random positions, so that fluctuations in δ_e resulted only from the patchiness of the reionization. In one case, the bubble radii were chosen from the size distribution predicted by our galaxy formation model. In the other case, all bubbles were given the same comoving radius of $0.62h^{-1}$ Mpc, which corresponds to the mean bubble radius (weighted by bubble volume) predicted by the galaxy model, at the redshift corresponding to the peak of the visibility curve. Both of these cases give power spectra with shapes (at large scales) similar to the analytical Gruzinov & Hu model, and completely different from when fluctuations in δ are included. In the final test (labelled “clustered” in right panel of Fig. 1), we again forced the bubble radii to be equal at a given redshift, but placed them on random halos, and included the fluctuations in the total gas density. The starting value for the radii in this last case was again $0.62h^{-1}$ Mpc, but the spheres were then grown by a uniform factor at each redshift to produce the correct mean ionized fraction, as in the model A. The power spectrum in this case is almost the same as in model A, showing that the distribution in bubble sizes in the latter case does not have much effect.

We conclude that in our model A, the *shape* of the power spectrum on scales large compared to the typical size of the ionized bubbles is determined primarily by the correlations in total gas density. However, in the case of *patchy* reionization, the *amplitude* depends on the spatial distribution of these patches, which produces *biasing* for the correlations in the ionized gas density relative to those in the total gas density, which in turn boosts the amplitude of the polarization fluctuations.

Finally, the second order power spectrum of polarization provides a very important constraint on the galaxy formation because their amplitude depends on models. A signal of this amplitude is below the detectability limits of the Planck Surveyor mission, which is the most accurate experiment in the near future. Therefore, detection of this signal should be a key aim of a post-Planck experiment with increased sensitivity and resolution in the next decade.

ACKNOWLEDGMENTS

We thank the Virgo Consortium for making available the GIF N-body simulations used here, and Shaun Cole, Carlos Frenk and Carlton Baugh for allowing us to use their model of galaxy formation. GCL thanks N. Seto for useful discussion. NS, AN and CGL acknowledge kind hospitality of Carlos Frenk and the physics department of University of Durham during the TMR network meeting. NS is supported by the Sumitomo foundation. CGL acknowledges support at SISSA from COFIN funds from MURST and from ASI. AN and AJB acknowledge the support of the EC RTN network “The Physics of the Intergalactic Medium”.

REFERENCES

1. Benson, A.J., Nusser, A., Sugiyama, N. & Lacey, C. G., 2001 MNRAS, 320, 153
2. Cole, S., Lacey, C. G., Baugh, C. M. and Frenk, C. S., 2000, MNRAS, 319, 168
3. Gruzinov, A. & Hu, W., 1998, ApJ, 508, 435
4. Shapiro, P. R., & Giroux, M. L., 1987, ApJ, 321, L107
5. Vishniac, E. T., 1987, ApJ, 322, 597